

# POROUS ARTIFICIAL REEFS: THE ROLES OF REFLECTION, BREAKING AND DRAG IN WAVE ATTENUATION

Justin Geldard, The University of Western Australia Coastal and Offshore Research Laboratory (CORL), [justin.geldard@research.uwa.edu.au](mailto:justin.geldard@research.uwa.edu.au)

Ryan Lowe, The University of Western Australia CORL, [ryan.lowe@uwa.edu.au](mailto:ryan.lowe@uwa.edu.au)

Scott Draper, The University of Western Australia CORL, [scott.draper@uwa.edu.au](mailto:scott.draper@uwa.edu.au)

Marco Ghisalberti, The University of Western Australia CORL, [marco.ghisalberti@uwa.edu.au](mailto:marco.ghisalberti@uwa.edu.au)

George Ellwood, The University of Western Australia CORL, [george.ellwood@uwa.edu.au](mailto:george.ellwood@uwa.edu.au)

Matthew Allen, MMA Offshore Limited, [matthew.allen@mmaoffshore.com](mailto:matthew.allen@mmaoffshore.com)

## INTRODUCTION

Artificial reef structures create habitat for marine organisms. However, they can also be designed to provide similar levels of coastal protection to natural reefs, as well as potentially more traditional engineered structures (e.g., submerged rubble mound breakwaters (Geldard et al. 2022)). Surface waves dissipate energy across submerged structures through a combination of (1) the partial reflection of waves offshore and (2) depth-limited wave breaking and, for reefs with high internal porosity, (3) dissipation by drag forces due to flows within the reef. For modular reefs where they can be separated into distinct reef rows, wave reflection can also be influenced by a combination of reflection from the offshore slope of the reef, as well as resonant interactions (Bragg scattering) of incident waves with the spacing of reef rows (e.g. Jeon & Cho (2006)). The contribution of each of these mechanisms to the overall wave attenuation will be influenced by geometric properties of the artificial reef, which will differ from submerged rubble mound breakwaters, as well as the wave and water level conditions.

The objective of this study was to explore the relationship between each wave attenuation mechanism and key hydrodynamic parameters as well as reef geometry (module shape and layout). An experimental study was undertaken with the MMA Offshore Bombora artificial reef modules in the University of Western Australia (UWA) Coastal and Offshore Research Lab (CORL) wave flume, formulating predictive tools and design frameworks for their use in coastal protection applications.

## EXPERIMENTAL TESTING

An in-depth physical modelling study was conducted to characterize wave attenuation over varying arrays of porous 1:5.8 scale Bombora artificial reef modules in the UWA CORL 54-m long, 1.5-m wide and 1.6-m deep wave flume. The scaled modules were cast from concrete and were approximately 310 mm tall with top and bottom diameters of 260 mm and 365 mm, respectively. The arrays tested had varying spacings between rows of modules, as shown in Figure 1.



Figure 1 - Photographs of wave interactions with different layouts of the modules tested with no spacing between rows (A) through to a spacing of three module diameters between rows (D).

Arrays of resistance-type wave gauges were located up-wave and down-wave of the reef to directionally separate incident, reflected and transmitted wave heights using a nonlinear 4 wave gauge approach (Andersen et al., 2017). Nortek Vectrino Acoustic Doppler Velocimeters were used to measure the instantaneous flow velocities experienced by a representative module located in the middle of each row across select layouts. The representative artificial reef modules were 3D printed which enabled them to be instrumented with a 3-axis 50 N load cell to also obtain the instantaneous hydrodynamic forces experienced by the modules.

Tests were conducted for each layout across various wave heights, periods and at three water depths to account for tidal variations in the water level above the modules. Each experiment lasted for 100 wave periods (3 - 10 minutes at model scale) to ensure that conditions in the flume reached a quasi-steady state.

## RESULTS

The different wave attenuation mechanisms were quantified in each test by coefficients for dissipation ( $K_A$ ), reflection ( $K_R$ ) and transmission ( $K_T$ ), defined as:

$$K_A = \sqrt{1 - K_T^2 - K_R^2} \quad (1)$$

$$K_T = H_t / H_i \quad (2)$$

$$K_R = H_r / H_i \quad (3)$$

where  $H_i$  and  $H_r$  are the decomposed offshore incident and reflected wave heights respectively, and  $H_t$  is the decomposed onshore transmitted wave height.

The relative freeboard, defined as the depth of water above the top of the reef ( $-R_C$ ) normalized by the incident offshore wave height, was the key governing parameter of the reefs' performance. This is demonstrated in Figure 2 for a subset of the tests (where the square of each coefficient, which relates to the distribution of wave energy, is shown).

The transmission of wave energy reduces significantly as the relative freeboard approaches zero, largely driven by an increase in dissipation by both wave breaking and drag forces (indicated by  $K_A^2$ ) (Figure 2). The independent contributions to  $K_A^2$  of wave breaking and drag force losses were decomposed using the measured horizontal flow velocities and drag forces experienced by the representative module in each row. From this, predictive tools were developed to estimate the initiation of wave breaking as well as total dissipation from drag forces across a variety of module layouts and wave climates.

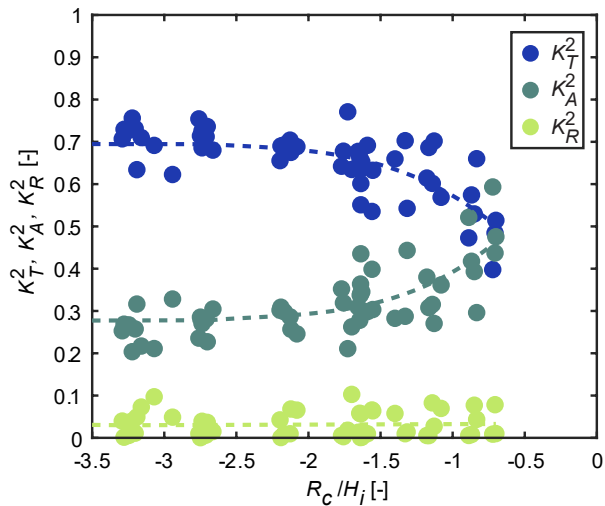


Figure 2 - Variation of the square of the transmission ( $K_T$ ), dissipation ( $K_A$ ) and reflection ( $K_R$ ) coefficients with the relative freeboard ( $-R_C/H_i$ ) for Layouts A and D in Figure 1.

The spacing between rows of modules ( $S$ ) relative to the incident wavelength ( $L$ ) is a second governing parameter of the reefs' performance and contributes to the scatter observed in Figure 2. While the reflection of wave energy does not significantly contribute to the overall attenuation in Figure 2, the contribution of reflection can become important through Bragg Scattering as the row spacing approaches half of the incident wavelength. This is demonstrated in Figure 3 where the wave condition was fixed and the spacing between rows was incrementally increased. The predictive tools for wave attenuation developed in this study therefore also incorporate the influence of the relative spacing, enabling a robust estimation of reef performance.

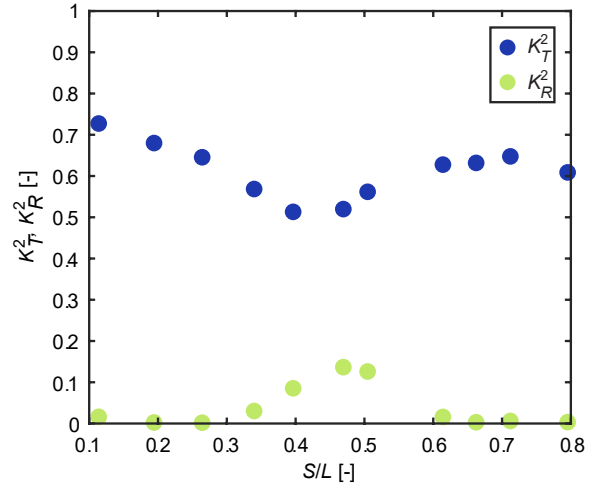


Figure 3 - Variation in the square of the transmission ( $K_T$ ) and reflection ( $K_R$ ) coefficients with the relative module row spacing ( $S/L$ ) for a fixed wave condition however varying the spacing between rows ( $S$ ).

SUMMARY

The contributions of reflection, wave breaking and drag force losses to wave attenuation over a porous artificial reef are evaluated here. Each mechanism is shown to depend on key hydrodynamic and reef geometric parameters. Quantification of these dependences allows development of predictive tools to optimize the performance of the reef in different design conditions. These tools can be used to motivate and incorporate artificial reef modules into nature-based solutions for coastal protection.

REFERENCES

Andersen, Eldrup & Frigaard, (2017): Estimation of incident and reflected components in highly nonlinear regular waves, Coastal Engineering, vol. 119, pp. 51-64.

Geldard, Lowe, Draper, Ellwood, Wood, Roe, Allen (2022): Performance of engineered wave attenuating reef structures, In Proceedings of Coasts & Ports 2021 Conference, New Zealand Coastal Society (11-13 April, Virtual).

Jeon & Cho (2006): Bragg reflection of sinusoidal waves due to trapezoidal submerged breakwaters, Ocean Engineering, vol. 33, pp. 2067-2082.

ACKNOWLEDGEMENTS

Funding by Australian Research Council Linkage Project (LP210100386), Australian Government Research Training Program Scholarship at The University of Western Australia, Keiran McNamara World Heritage PhD Top-Up Scholarship at The University of Western Australia and MMA Offshore.